Global statistics of lightning in anvil and stratiform regions over the tropics and subtropics observed by the Tropical Rainfall Measuring Mission

Michael Peterson[1] and Chuntao Liu[1]

Received 4 March 2011; revised 15 September 2011; accepted 15 September 2011; published 2 December 2011.

[1] The statistics of lighting in the anvil and stratiform regions of convective systems are summarized from Tropical Rainfall Measuring Mission (TRMM) satellite observations from 1998 to 2009. The locations of lightning flashes in convective systems are determined by combining three-dimensional precipitation radar (PR) observations with lightning flash center locations from lightning imaging sensor observations. The geographical distributions of flashes in the anvil and stratiform regions of thunderstorms over the tropics and subtropics are presented. Flashes in stratiform regions are found to account for 5.6% of all lightning flashes observed within the TRMM PR swath, while flashes in nonraining anvil regions made up another 5.5% of the sample. Diurnally, flashes in anvil regions peak earlier than flashes in stratiform regions (15:30 LT as opposed to 17:30 LT). Seasonal and regional variations of these flashes are discussed. Features in PR observations that likely contribute to charge separation are identified as contiguous areas with 6 km echoes exceeding 30 dbZ. Lightning flashes are then assigned to one of these features by the nearest neighbor method. Convective properties of features linked with lightning in stratiform and nonraining anvil regions are then analyzed. We find that features associated with lightning flashes in anvil regions are relatively weak and occur in small systems composed of a single convective region, while flashes in the stratiform regions are also relatively weak but more likely occur in multicell systems. About 15% of features with lightning are associated with at least one stratiform or anvil flash.

Citation: Peterson, M., and C. Liu (2011), Global statistics of lightning in anvil and stratiform regions over the tropics and subtropics observed by the Tropical Rainfall Measuring Mission, *J. Geophys. Res.*, *116*, D23201, doi:10.1029/2011JD015908.

1. Introduction

[2] Linking storm structure and lightning activity is by no means a new idea. *Battan* [1964] noted that the atmospheric properties that control the updraft also control lightning and precipitation, and since the dawn of the golden era of operational weather radar, a multitude of studies have examined correlations between radar reflectivity and lightning initiation. Empirical relationships have been found between sferics rates and plan view areas exceeding specific reflectivity thresholds for both 43 dbZ at 7 km [*Larsen and Stansbury*, 1974] and 30 dbZ at 6 km [*Marshall and Radhakant*, 1978].

[3] Since then, a number of studies have been carried out to examine the coupling between storm structure and electrical activity for storms in both the midlatitudes [*Bruning et al.*, 2007; *Lund et al.*, 2009], and the tropics [*Petersen et al.*, 2005; *Carey and Rutledge*, 2000], as well as for specific types of storms including mesoscale convective systems [*Keighton et al.*, 1991; *Carey et al.*, 2005; *Dotzek et al.*, 2005; *Ely et al.*, 2008; *Lang and Rutledge*, 2008] and supercells [*Bluestein and MacGorman*, 1998; *MacGorman et al.*, 2005].

[4] One area that has received less attention is lightning production in the stratiform and anvil regions of storms, though many advances have been made in recent years. Flashes in these regions are rare compared to those in the convective regions of storms, and are often the result of complex charge structures and charging mechanisms, making them difficult to study. Furthermore, because they have been observed to propagate over large distances [*Lang et al.*, 2004, 2010; *Lang and Rutledge*, 2008; *Ely et al.*, 2008; *Kuhlman et al.*, 2009; *Stolzenburg et al.*, 2010], these flashes can be particularly dangerous, especially for aviation. Thus, it is important to study these types of lightning flashes and the structure of the storms in which they occur.

[5] While the stratiform region is technically an extension of the anvil region, the charging mechanisms available to regions with stratiform precipitation are likely to be different than those in the convective anvil. The convective anvil is thought to accumulate charge primarily through advection from the convective core, though other sources of charge, including in situ generation, cannot be ruled out at this time. Charge advection into the anvil is not necessarily continuous,

[1]Department of Atmospheric Sciences, University of Utah, Salt Lake City, Utah, USA.

0148-0227/11/2011JD015908

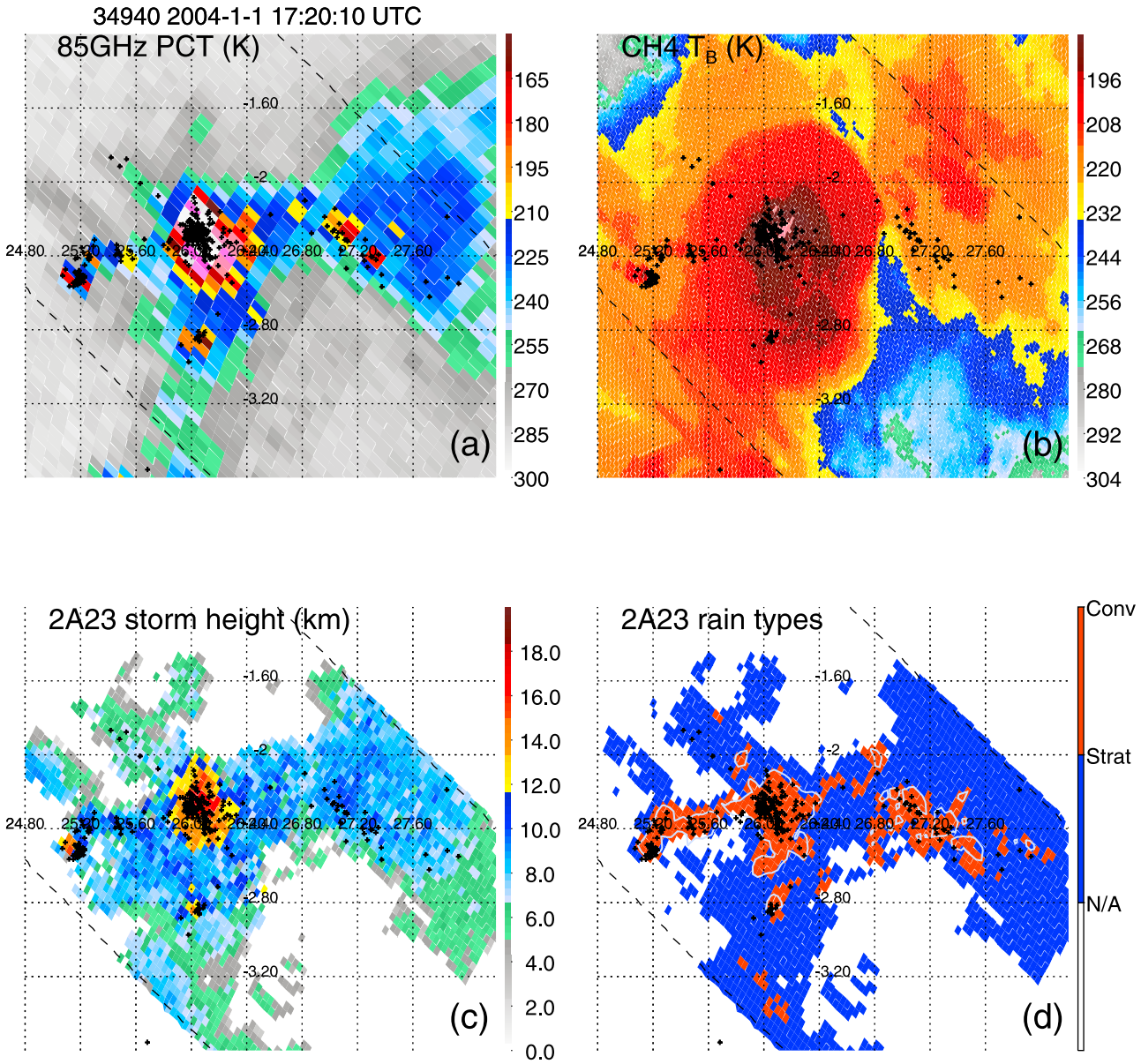

Figure 1. An example of the locations of lightning flashes (black dots) in a mesoscale convective system over central Africa in 2004. (a) TRMM TMI 85 GHz polarization-corrected temperature. (b) VIRS infrared brightness temperature. (c) PR echo-top height. (d) PR 2A23 convective/stratiform classification. Areas with PR reflectivity >30 dbZ at 6 km are outlined with a white solid line. Note that most lightning flashes are within convective areas, but there are a few flashes in the stratiform region.

and does not occur everywhere within the anvil region [*Dye et al.*, 2007]. Furthermore, accumulation of significant amounts of positive charge within convective anvils may result in negative screening layers near the upper and lower boundaries of the cloud [*Marshall et al.*, 1989], resulting in an even more complex charge structure.

[6] Unlike the convective anvil, the stratiform region has precipitation extending below the melting level, and is thought to accumulate charge by both advection from the convective core and in situ charge generation [*Rutledge and MacGorman*, 1988], which may be enhanced by mesoscale updrafts within the stratiform region [*Ely et al.*, 2008; *Lang and Rutledge*, 2008]. These processes result in a horizontally extensive layered charge structure that can exceed 100 km across that is thought to serve as a conduit for lightning propagation [*Marshall and Rust*, 1993; *Stolzenburg et al.*, 1994; *Lang et al.*, 2004; *Marshall et al.*, 2009]. As many as 6 of these vertically stacked charge layers have been observed in nature, and it has been suggested that the uppermost three are primarily the result of charge advection while the lowest two are likely the result of in situ generation [*Schuur and Rutledge*, 2000].

[7] Until recently, the primary means of conducting lightning research has been through the use of ground-based radars and lightning detection networks. While radar studies have produced incredibly useful results and insights into the evolution of the electrical and precipitation structures of storm systems throughout the courses of their lives, these

studies lack a global perspective and large number of cases to ensure a representative sample. One way to fill in these gaps is through the use of satellite data. The Tropical Rainfall Measuring Mission (TRMM) satellite is particularly well equipped to study lightning storms worldwide. Its sensor package includes the Precipitation Radar (PR), the TRMM Microwave Imager (TMI), the Visible and Infrared Scanner (VIRS) and the Lightning Imaging Sensor (LIS), which allow for the detailed analysis of storms from space [*Kummerow et al.*, 1998]. Using these sensors, it is possible to compare the convective structure of storms and the lightning they produce in different regions of the tropics and the subtropics between 36°N and 36°S latitude. Results from TRMM have the benefit of providing a global perspective to lightning research [*Christian et al.*, 2000; *Boccippio et al.*, 2002; *Cecil et al.*, 2005; *Petersen et al.*, 2005], even though TRMM lacks the ability to examine charging mechanisms and charge structure directly.

[8] A number of studies have used TRMM observations to examine relationships between lightning production and various storm parameters, such as ice water path estimated from PR reflectivity [*Petersen et al.*, 2005], maximum PR reflectivity and minimum TMI brightness temperatures [*Cecil et al.*, 2005], rain yield for storms in the tropics [*Takayabu*, 2006], and volume of intense convection in storms in southeast Asia [*Xu et al.*, 2010]. However, these studies did not take into consideration the locations in which lightning flashes occurred with respect to storm structure. There has also not yet been a study on the global statistics of lightning flashes in the stratiform and anvil regions, specifically. Moreover, these studies attempt to relate lightning production to the properties of the entire precipitation system. However, in order to explain each flash in a large storm, such as the multicellular mesoscale convective system (MCS) in central Africa shown in Figure 1, the properties of the nearby convective regions are likely more important than the maximum convective intensity of the entire system.

[9] This study seeks to provide a global set of statistics of lightning flashes in the stratiform and anvil regions of storms using 12 years (1998–2009) of TRMM observations. Though it is impossible to determine with complete certainty which convective regions are responsible for which lightning flashes in many cases owing to the inability of TRMM to observe individual systems for significant lengths of time, it is still useful to examine the properties of convective regions near lightning. Areas likely contributing to charge separations are identified using PR observations and their properties are also presented.

2. Data and Methods

[10] The first challenge in this study is to create systematic definitions for identifying stratiform and anvil lightning, as well as areas likely contributing to charge separation. The locations of lightning flashes are defined as their centers of illumination as observed by the LIS. This, of course, can be problematic owing to the 90 s view time of the LIS, and for flashes that propagate over large distances. Nonetheless, this definition allows lighting flashes to be collocated with PR pixels, which then make it possible to analyze lightning flashes relative to the structure of the parent storm. Convective and stratiform regions are classified using the PR 2A23 algorithm, which uses both vertical and horizontal PR reflectivity gradients [*Awaka et al.*, 1998] to differentiate between each type of precipitation. In order for a lightning flash to be considered a stratiform flash, its center must be collocated to a PR pixel that is considered stratiform by the 2A23 algorithm, and rain must be detected near the surface. Anvil flashes, however, are defined as lightning flashes collocated to a PR pixel where there is no precipitation detected near the surface, regardless of the 2A23 precipitation type of that pixel. Near-surface rain rates are calculated by the 2A25 TRMM algorithm, which can detect rain rates greater than 0.1 mm/h [*Iguchi et al.*, 2000].

[11] Even though there is no 2A23 rain type requirement for anvil flashes, the requirement that stratiform flashes must have rain detected near the surface ensures that there is no overlap between the two groups. This can lead to misclassification errors, however. Since the LIS observation window is only 90 s, it is possible for lightning to be detected in a region where stratiform rainfall has not yet reached the ground. Misclassification errors can also arise in cases of dissipating or noncontiguous stratiform precipitation. In order to get a handle on how frequent these types of errors are, the stratiform fraction of the area within a 10 km radius of each flash is computed to identify anvil flashes embedded in areas dominated by stratiform precipitation. Only 8% of anvil flashes are found in regions identified as primarily (>80%) stratiform by the 2A23 rain type algorithm. However, many of these are regions with no surface rainfall that are classified as stratiform by the 2A23 algorithm, so the true number of misclassified flashes is probably significantly smaller than this 8%. Regardless, removing these flashes from the anvil flash sample does not appear to alter the overall statistics.

[12] Because anvil flashes are defined as those with no detectible rainfall near the surface, some additional quality controls must be performed on the sample. The LIS has a problem with interference from the South Atlantic Anomaly [*Boccippio et al.*, 2002], which results in random artifacts. Most of these artifacts can be removed by requiring nonzero near-surface rain rates, but there is no systematic way to distinguish between real flashes and artifacts on a flash-by-flash basis. For this reason, it is necessary to remove all anvil flashes in the affected region. Global statistics of lightning based on these definitions and filters are presented in sections 3.1 and 3.3.

[13] Areas likely to contribute to charge separation are then identified from PR data on the basis of methods used in previous studies relating lightning production with reflectivity thresholds at arbitrary altitudes within the mixed-phase region [e.g., *Larsen and Stansbury*, 1974; *Marshall and Radhakant*, 1978]. These features, known as Larsen areas, are good indicators of lightning because moderate-to-high reflectivity in this region signifies the presence of graupel, which is important for the noninductive charging mechanism [*Takahashi*, 1978; *Jayaratne et al.*, 1983; *Saunders et al.*, 1991]. Multiple combinations of altitudes and reflectivity thresholds have been used in previous research, but for this study, a suitable Larsen area definition should retain most relatively weak convective areas that might be, or might have been, significant sources of charge, while omitting most stratiform precipitation. For this reason, we chose to

Table 1. Global Statistics of All Lightning Within the PR Swath Between 36°N and 36°S Characterized by Type From Observations Between 1998 and 2009[a]

	Global		Land Only		Ocean Only	
	Count	%	Count	%	Count	%
All	5,934,492		4,840,322		1,094,205	
Anvil	324,052	5.46	266,894	5.51	57,160	5.22
Stratiform	334,660	5.64	251,818	5.20	82,844	7.57
Inside Larsen areas	4,135,403	69.68	3,457,971	71.44	673,344	61.54

[a]Here Larsen areas are defined by areas with >30 dbZ at 6 km. These statistics are normalized by total sampled pixels at different latitudes to counteract sampling bias. Anvil flashes over Argentina are not included owing to the large interference from the South Atlantic Anomaly.

use the threshold suggested by *Marshall and Radhakant* [1978] of 30 dbZ at 6 km as the basis of our Larsen area definition. Using an algorithm similar to the one used by *Liu and Zipser* [2008] for the precipitation feature database, Larsen areas are identified by grouping contiguous pixels with echoes exceeding 30 dbZ at 6 km using 12 years of PR reflectivity data. The characteristics of these Larsen areas are then calculated, including size, shape, and a number of convective proxies derived from PR, TMI, VIRS, and LIS data.

[14] Perhaps the biggest problem with constant-altitude Larsen area definitions is that it does not work very well in the case of wintertime subtropical lightning storms due to the lower height of the melting layer during the cold season. A better approach would be to create a definition using radar reflectivity threshold at a specific temperature level using reanalysis data. However, since the primary focus of the TRMM satellite is the tropics, and the amount of lightning from these winter storms only makes up a small percentage of the total sample, it is adequate to use our constant-altitude Larsen area definition and then filter out these wintertime subtropical Larsen areas. In the subsequent sets of Larsen area statistics, Larsen areas north of 20°N between the months of October and April and south of 20°S between the months of April and October have been excluded from the sample.

[15] The Larsen area closest to, or containing, each individual lightning flash is then identified using the nearest neighbor method, and statistics of flashes associated with Larsen areas are computed. While it is possible for flashes to span great distances, most flashes occur close to Larsen area centers. Even for stratiform flashes, less than 20% are centered more than 30 km from Larsen area centers. A more in-depth study would be required to differentiate between flashes initiating in the convective core, and those occurring deep in the heart of the stratiform region. Because some lightning flashes in the stratiform and anvil regions are likely caused by local processes, relating stratiform and anvil lightning flashes to the nearest Larsen areas may not be appropriate. The focus here is to simply present the statistics of the properties of convective regions near each type of lightning flash.

[16] Of course, the nearest neighbor method also has the potential to induce errors, particularly in cases of closely spaced Larsen areas, small Larsen areas within the stratiform region, and lightning flashes right at the edge of the PR swath or where there are missing PR data. However, these errors can be reduced by filtering out Larsen areas smaller than 4 PR pixels (~80 km^2) and lightning flashes at exceptionally large distances (>200 km) away from Larsen area centers. These two filters are only used in sections 3.4 and 3.5, which discuss Larsen areas and the lightning associated with them. Despite these restrictions, more than 3.9 million flashes remain in the sample, which is 64% of the original sample size. Statistics of the properties of the Larsen area associated with different types of lightning flashes are discussed in sections 3.4 and 3.5.

3. Results

3.1. Global Statistics of Stratiform and Anvil Lightning

[17] The global statistics of stratiform and anvil flashes from 1998 to 2009 are summarized in Table 1. At this stage, the only filters that have been applied are the removal of anvil flashes over Argentina to avoid interference from the South Atlantic Anomaly, and the requirement that each flash must lie within the PR swath. The sample is also normalized by latitude in order to account for oversampling in the subtropics. Anvil and stratiform flashes make up only a small fraction of the total amount of lightning observed globally, and anvil flashes appear to be slightly less common than stratiform flashes overall. This is at least in part due to the removal of Argentina, one of the world's most electrically active regions.

[18] Despite the fact that 82% of flashes occur over land, there is little difference in the fraction of anvil flashes between land and ocean. Stratiform flashes, however, make up a higher fraction of flashes over the ocean, even though more stratiform flashes are still observed over land. Most lightning flashes occur in areas meeting our Larsen area definition, however flashes over the ocean are somewhat less likely to occur in these regions.

[19] Despite accounting for less than 6% of the world's lightning flashes each, stratiform and anvil flashes are not so uncommon everywhere. Figure 2 shows the global distribution of lightning flashes (Figure 2a) and the relative fraction of and flashes in areas not meeting Larsen area definition (Figure 2b), stratiform flashes (Figure 2c), and anvil flashes (Figure 2d). As seen in Figure 2b, flashes outside of Larsen areas are common over certain regions, particularly in the subtropics. This is likely due to problems with our constant-altitude Larsen area definition during the winter, discussed previously.

[20] While the global distributions of stratiform and anvil flashes closely mirror the distribution of all flashes, Figures 2c and 2d show regions of the world where these types of flashes make up a significant fraction of all observed lightning. Oceanic regions tend to have higher

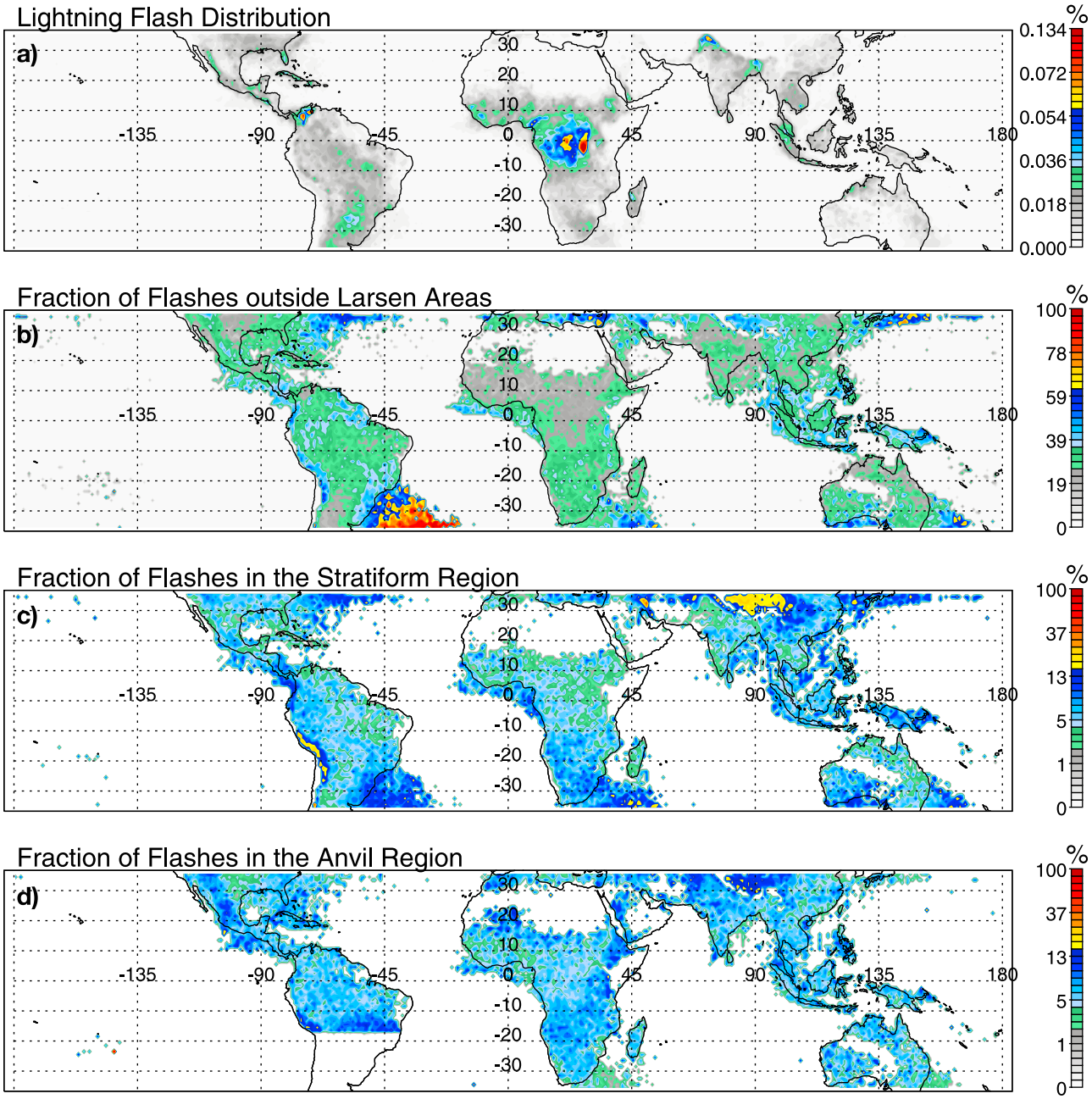

Figure 2. Global distribution of (a) lightning flashes and (b) the fractions of flashes in regions that do not meet the 30 dbZ at 6 km Larsen area definition, (c) flashes in the stratiform region, and (d) anvil lightning flashes in 1° by 1° bins. Bins with insignificant numbers of flashes are set to 0 in Figures 2b, 2c, and 2d. Note that, owing to a lack of PR observations over central-west Australia, no flashes are shown in this region.

fractions of stratiform lightning than land-based regions, sometimes as high as 20% in some areas. Many of these regions also tend to be downwind of major continents in the subtropics, which is consistent with the results from *Christian et al.* [2003]. The high fractions of stratiform flashes in these regions are likely the result of local weather regimes. The northern Pacific, for instance, is famous for its winter thunderstorms [*Yamamoto et al.*, 2006], which often result from cold air outbreaks from over Siberia and mid-latitude cyclones. Stratiform lightning also accounts for a high fraction of lightning in high-terrain regions, but this is most likely due to incorrect stratiform pixel differentiation by the 2A23 algorithm [*Fu and Liu*, 2007]. The total number of stratiform flashes in these regions, however, is small and therefore these errors do not significantly affect the global statistics.

[21] Anvil flashes also account for a high fraction of lightning in high-terrain regions such as the Andes, Rockies and Himalayas, as well as certain desert regions, including parts of Mali, Niger, Algeria, and Saudi Arabia (Figure 2d).

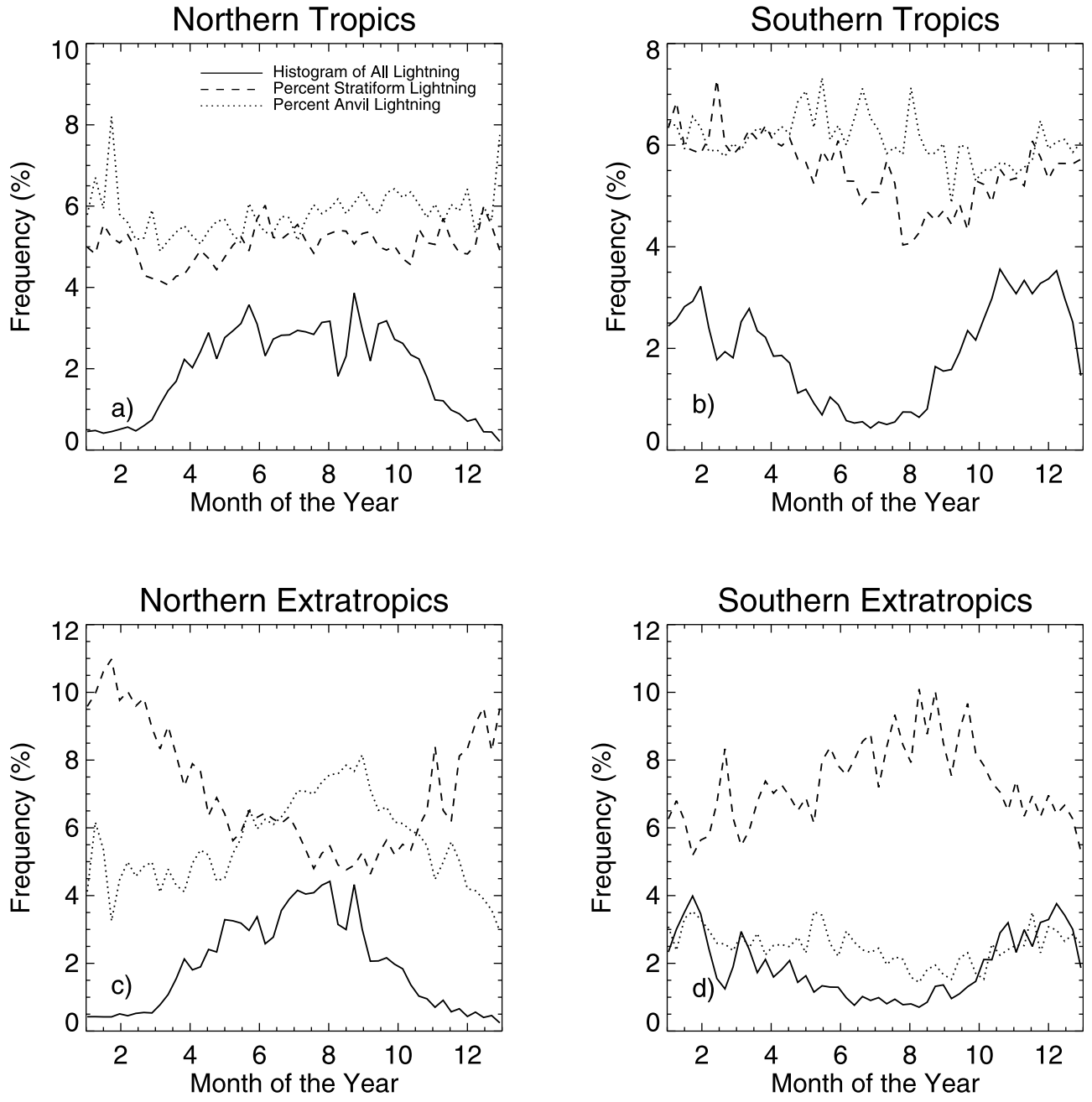

Figure 3. Weekly variation of the frequency of lightning flashes and the regional fractions of stratiform and anvil flashes for (a) the Northern Hemisphere tropics (0°–20°N), (b) the Southern Hemisphere tropics (0°–20°S), (c) the Northern Hemisphere extratropics (20°–36°N), and (d) the Southern Hemisphere extratropics (20°–36°S).

While lightning flashes in these regions are quite uncommon, about 15% of all flashes in these regions are identified as anvil flashes. This could be due to the presence of large anvil clouds in early stages of convection in high-terrain regions, or the evaporation of rain before it reaches the ground in arid regions.

3.2. Seasonal and Diurnal Variations of Stratiform and Anvil Lightning

[22] Figure 3 shows a histogram of lightning production and the fractions of stratiform and anvil flashes throughout the year in four different regions. As seen in Figures 3a and 3b, the fractions of stratiform and anvil lightning remain fairly constant year-round in the tropics, only varying by 1–2%. In contrast, there is a more pronounced seasonal cycle in the subtropics.

[23] In both hemispheres, stratiform lightning accounts for the highest percentage of winter lightning, which likely includes lightning in snowstorms [*Schultz*, 1999], and is lowest during the summer months. In contrast, anvil flashes account for a higher fraction of summer lightning and a smaller fraction of winter lightning in the Northern

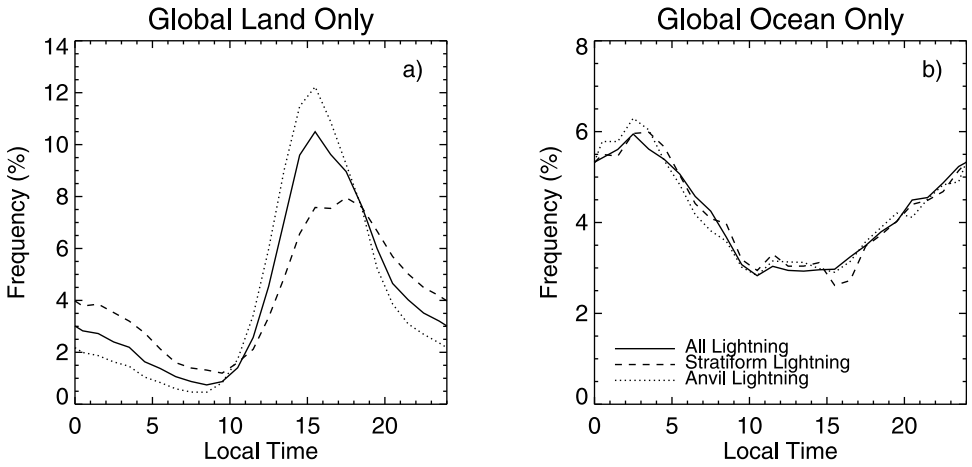

Figure 4. Diurnal cycles of all lightning, stratiform flashes, and anvil flashes over (a) land and (b) oceans.

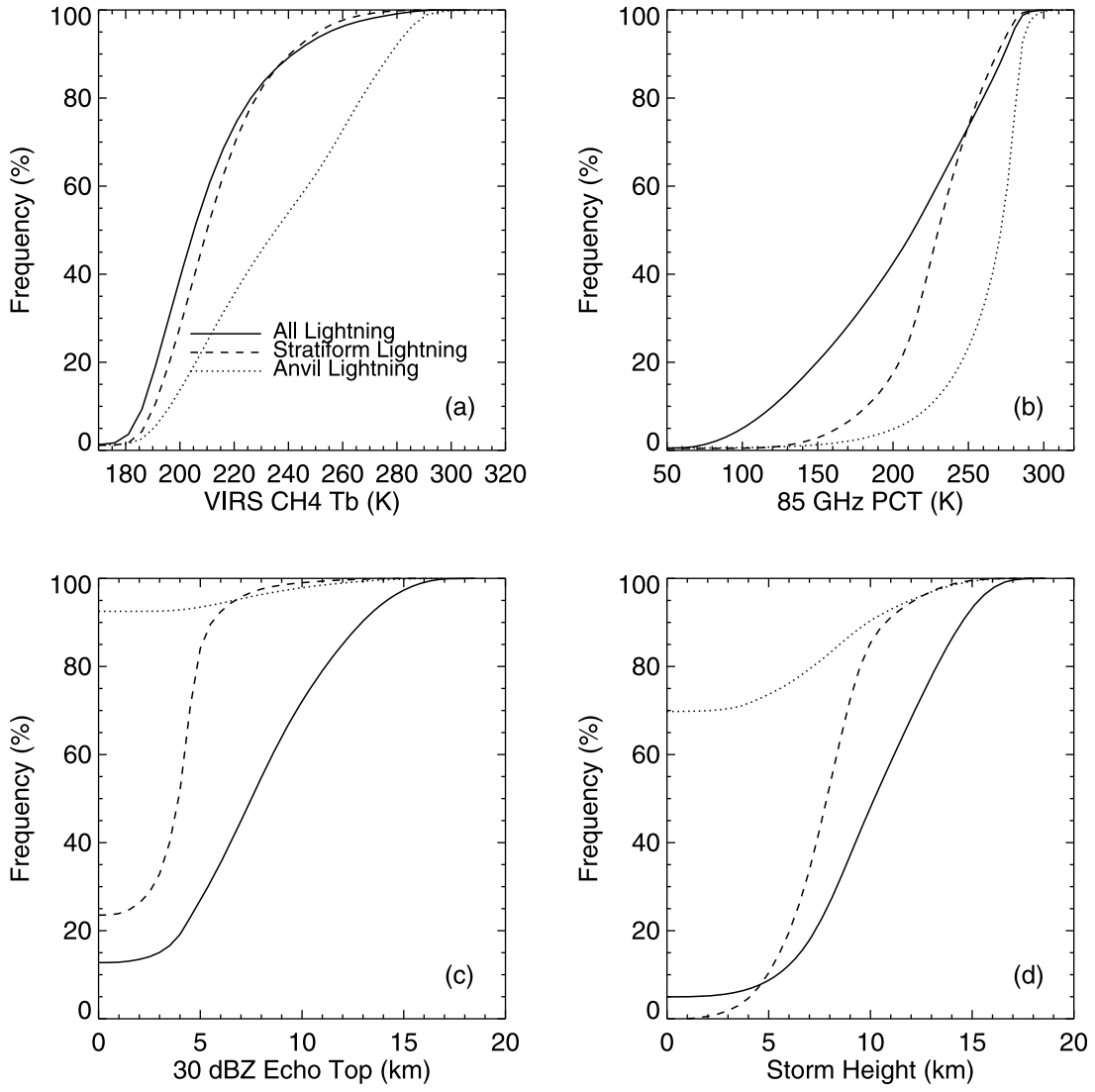

Figure 5. Cumulative distribution functions of VIRS, PR, and TMI observations at the center locations of lightning flashes. (a) VIRS channel 4 infrared brightness temperature. (b) The 85 GHz polarization-corrected temperature. (c) Maximum height of the 30 dbZ echo. (d) Echo-top height.

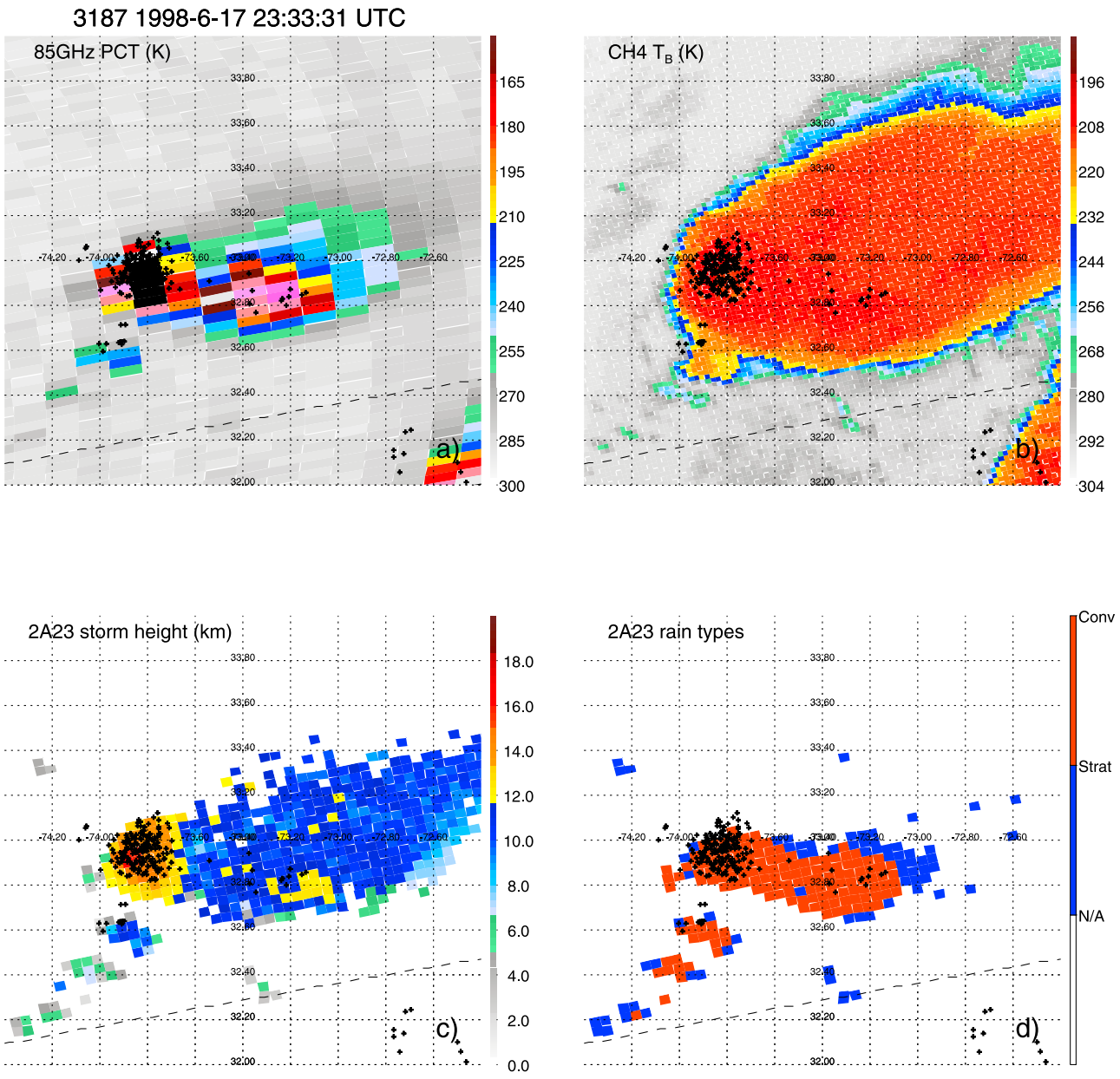

Figure 6. An example of a thunderstorm with anvil flashes occurring in regions with no PR echo over north Atlantic in June 1998. (a) TRMM TMI 85 GHz polarization-corrected temperature. (b) VIRS infrared brightness temperature. (c) The 2A23 storm. (d) PR 2A25 near-surface rain rate.

Hemisphere. In the Southern Hemisphere, however, the anvil lightning fraction changes little throughout the year, though anvil flashes do account for a slightly higher fraction of lightning between November and April than during the rest of the year.

[24] Figure 4 shows the diurnal cycles of each type of lightning over land and over the ocean. There is a 12 h lag between the peaks of land-based and oceanic lightning, which is consistent with typical diurnal cycles of convection and lightning seen in previous studies [*Hendon and Woodberry*, 1993; *Nesbitt and Zipser*, 2003; *Liu and Zipser*, 2008]. While there is little difference between the diurnal cycles of all lightning, stratiform lightning, and anvil lightning over the ocean, there are significant differences in the diurnal cycles of each type of lightning over land. The diurnal cycle for anvil flashes over land peaks at roughly the same time as all lightning in general, and anvil flashes are relatively more common during the early afternoon, less common in the morning, and have the largest amplitude of diurnal variation. The diurnal cycle for stratiform flashes over land peaks almost 2 h later than that for anvil lightning (17:30 compared to 15:30, local time). Stratiform flashes are the least common type in the early afternoon, the most common type overnight and into the morning, and have the weakest diurnal cycle amplitude. This is consistent with the life cycles of the MCSs seen in earlier studies [e.g., *Nesbitt and Zipser*, 2003; *Liu and Zipser*, 2008].

Table 2. Global Statistics of Lightning Flashes Associated With Larsen Areas and Larsen Areas With Lightning Between 36°N and 36°S Excluding Wintertime Subtropical Storms Normalized by Latitude[a]

	Flashes Associated With Larsen Areas		Larsen Areas With Lightning	
	Count	%	Count	%
All	4,086,599		534,843	
Anvil	200,547	4.91	94,758	17.72
Stratiform	158,376	3.88	82,134	15.36
Inside Larsen areas	2,938,682	71.91	434,553	81.25

[a]Greater than 20° latitude. Flashes farther than 200 km from Larsen area centers and anvil flashes over Argentina are not included in this sample.

3.3. Convective Properties at Flash Locations

[25] The statistics of a number of convective properties at the locations of lightning flashes of each type are presented in Figure 5. There is only a slight difference between the VIRS channel 4 infrared brightness temperature distributions for all lightning and stratiform flashes (Figure 5a), but anvil flashes are significantly warmer than the other two groups. Both stratiform and anvil flashes tend to have relatively warm polarization-corrected temperatures (PCTs) [*Spencer et al.*, 1989] (Figure 5b) compared to all lightning, with anvil flashes associated with the warmest PCTs, corresponding to the smallest column ice contents.

[26] Part of this trend could be the fact that the TMI has a larger footprint than the PR, leading to collocation errors, as well as beam filling in the case of steep PCT gradients, such as near the edges of storms. However, PR-based convective proxies also show significant differences between stratiform and anvil flashes. More than 90% of anvil flashes are centered in regions with no 30 dbZ echoes (Figure 5c), and up to 70% of anvil flashes have no PR reflectivity anywhere in the column (Figure 5d). This is most likely because the PR cannot detect reflectivities less than ~17 dbZ in thin anvil clouds. The remaining 30% of anvil flashes occur in areas where there are detectable PR echoes, corresponding to thicker anvil clouds, and roughly one-third of these have echoes exceeding 30 dbZ, and may eventually produce stratiform precipitation.

[27] While the sensitivity of the PR is likely the primary cause for most of these flashes being centered in regions with no echo, there are other situations that can produce similar results. Figure 6 shows a storm over the northern Atlantic in 1998 with two convective regions. A number of anvil flashes are present in this case, including three near the northwest edge of the convective system with infrared brightness temperatures exceeding 270 K and 85 GHz PCTs exceeding 250 K (Figures 6a and 6b). These flashes could be LIS artifacts. There are also two flashes occurring between the two convective regions. These flashes could possibly be large lightning flashes propagating between two separate charge regions. Furthermore, there are also a number of anvil flashes along the northern edge of the system centered in regions with no PR echo. These flashes could have no PR echo owing to the coarse spatial resolution of the PR, or inadequacies of determining flash location as the center of illumination (Figure 6c). However, given the fact that the cirrus cloud shield extends well beyond the locations of these flashes, they likely occur in thin anvil clouds, where reflectivities are less than 17 dbZ.

3.4. Convective Properties of Larsen Areas Close to Anvil and Stratiform Lightning

[28] To study the characteristics of Larsen areas associated with stratiform and anvil lightning, a subset of the data is used that is subject to additional quality control filters. Only lightning flashes associated with a Larsen area greater than 4 PR pixels in size and that occurred within 200 km of the nearest Larsen area center are considered. Also, Larsen areas and lightning flashes observed during the winter poleward of 20° latitude are omitted. The global statistics of the remaining flashes and Larsen areas are summarized in Table 2. In this new sample, the shares of stratiform and anvil flashes have been reduced, mostly owing to the 4 PR pixel Larsen area size constraint. The greatest reduction is in the fraction of stratiform flashes, which fell from 5.64% to just 3.88%. At the same time, a greater percentage of flashes in this sample are centered in areas with echoes exceeding 30 dbZ at 6 km. Despite these changes, 15–17% of Larsen areas with lightning are found to be associated with at least one anvil or stratiform flash. Thus, stratiform

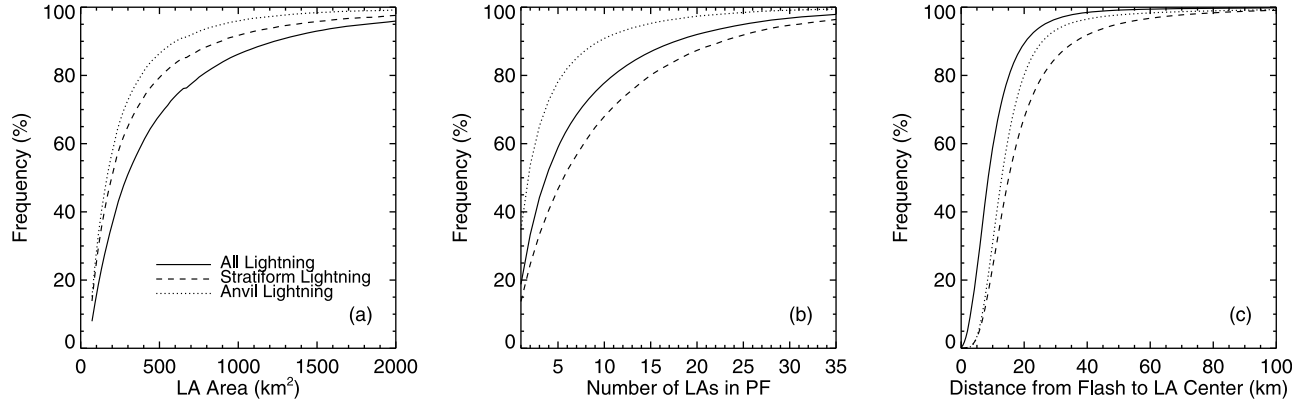

Figure 7. Cumulative distribution function of the properties of Larsen areas associated with lightning in the TRMM domain, excluding those in the subtropics during the winter. (a) Larsen area size. (b) Number of Larsen areas in the contiguous precipitation region. (c) Distance from each flash to the Larsen area center.

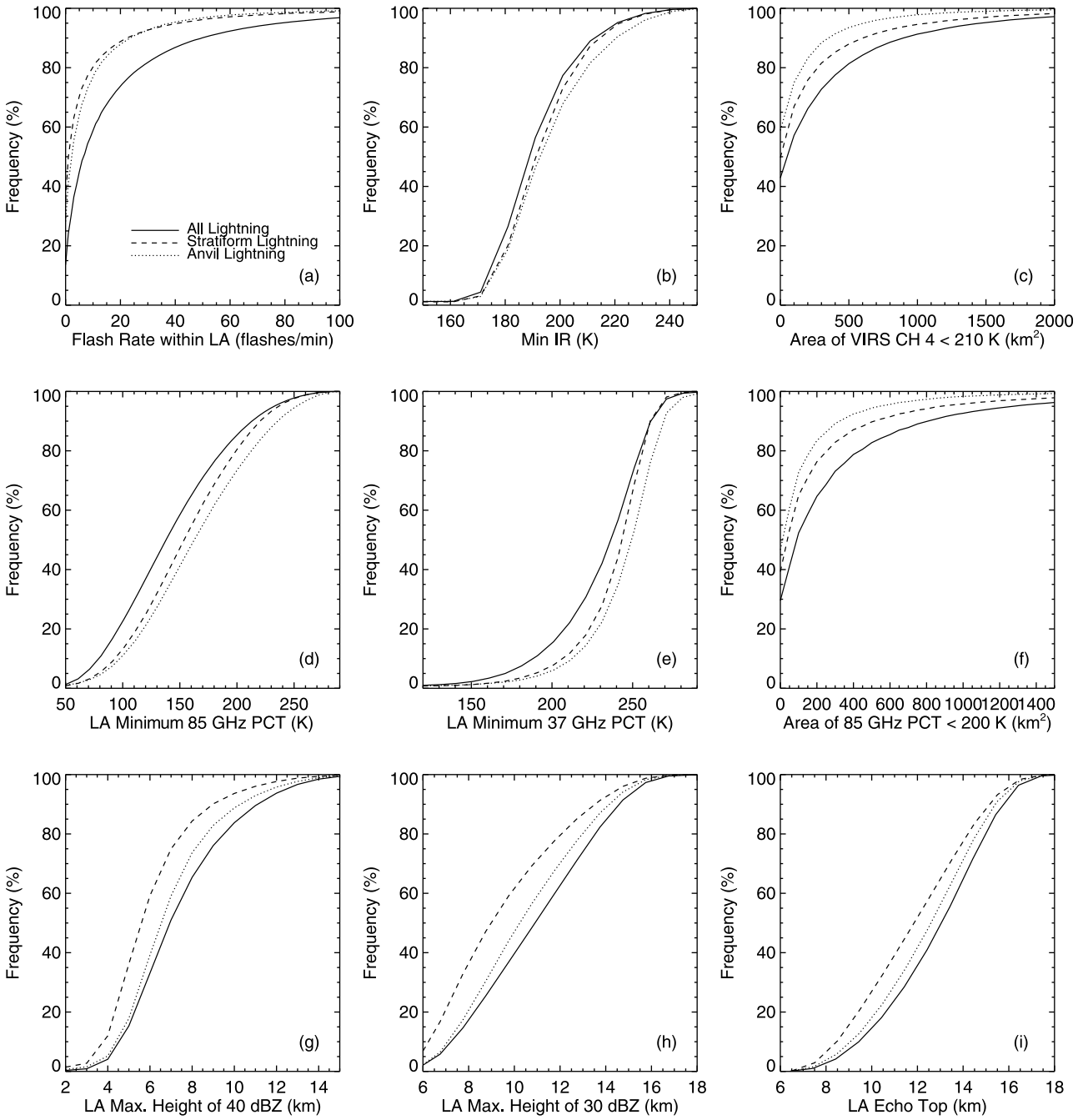

Figure 8. Cumulative distribution functions of some convective properties of Larsen areas associated with lightning in the TRMM domain, excluding those in the subtropics during the winter. (a) Flash rate inside the Larsen area. (b) Minimum VIRS infrared temperature T_{B11}. (c) Area with VIRS T_{B11} <210 K. (d) Minimum 85 GHz PCT. (e) Minimum 37 GHz PCT. (f) Area with 85 GHz PCT <200 K. (g) Maximum height of the 40 dbZ echo. (h) Maximum height of the 30 dbZ echo. (i) Maximum echo-top height.

and anvil flashes are not necessarily uncommon, but they occur in smaller numbers than other types of lightning.

[29] Figure 7 examines the physical characteristics of Larsen areas associated with each type of lightning. Since the sample is dominated by Larsen areas with only a single flash, the histograms of each type of lightning in Figures 7 and 8 have been weighted by that the number of flashes of each type associated with a particular Larsen area. As seen in Figure 7, Larsen areas with anvil flashes tend to be relatively small and occur in systems that are generally composed of a small number of Larsen areas. In fact, as many as 35% of anvil flashes occur in single-cell systems, compared to 18% for stratiform flashes. Over half of stratiform flashes occur in systems consisting of more than 5 Larsen areas (Figure 7b). Larsen areas with stratiform flashes also tend to be smaller than average (Figure 7a), yet stratiform flashes tend to occur at greater distances from the Larsen area center than other types (Figure 7c). Even though roughly 80% of anvil flashes

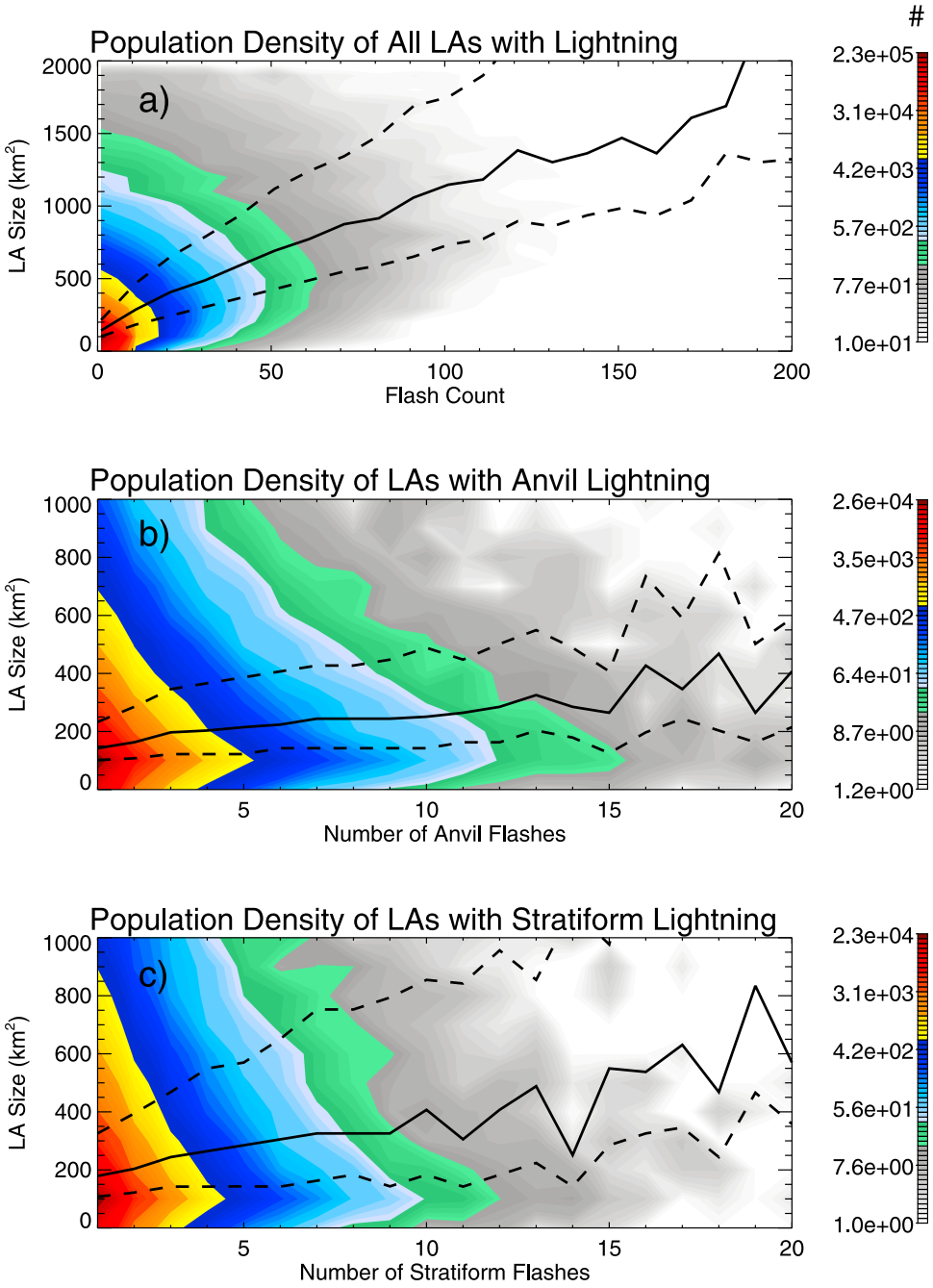

Figure 9. Two-dimensional histograms of Larsen areas (LAs) with lightning categorized by size and number of flashes with bin sizes 20 km^2 and variable flash counts, excluding samples observed during the cold season in the subtropics. (a) Larsen areas with flashes with 10 flash bins. (b) Larsen areas with anvil lightning flashes with 1 flash bins. (c) Larsen areas with stratiform lightning flashes with 1 flash bins. Color contours represent the number density of Larsen areas in each bin. The median, 25th, and 75th percentiles of Larsen area size for each flash count bin are overlain.

occur within 20 km of the center of the Larsen area, distant anvil flashes are nonetheless present in these statistics.

[30] The statistics of a number of convective properties of Larsen areas associated with each type of lightning are shown in Figure 8. In nearly 30% of Larsen areas with either anvil or stratiform flashes, no flashes are observed inside the Larsen area (Figure 8a), possibly due to the 90 s sampling time of the LIS. Also, Larsen areas that are associated with stratiform or anvil lightning tend to have slightly warmer VIRS infrared brightness temperatures and significantly smaller areas of cold cloud-top temperatures than Larsen areas with lighting, in general, as seen in Figures 8b and 8c.

[31] Figures 8d, 8e, and 8f show the statistics of three TMI-based convective intensity proxies for Larsen areas. While Larsen areas with both stratiform or anvil flashes tend to be weaker than average, Larsen areas with anvil flashes

tend to have the warmest PCTs. PR-based convective proxies tell a slightly different story, however. The maximum heights of the 40 and 30 dbZ echoes within the Larsen areas, shown in Figures 8g and 8h, as well as maximum echo-top height, shown in Figure 8i, indicate that Larsen areas with stratiform flashes tend to be weaker than even those with anvil flashes, corresponding to lower echo-top heights.

3.5. Correlations Between Convective Proxies of Larsen Areas and Lightning Frequency

[32] While the closest Larsen area may not be the primary source of charge separation for many lightning flashes, particularly those in the stratiform and anvil regions, the intensity of nearby convection may still be an indicator of different levels of lightning activity. Figure 9 shows a 2-D histogram of Larsen area size and flash count for each type of lightning. The median, 25th and 75th percentiles of the sizes of Larsen areas with incremental flash counts are also overlain. While there appears to be a relationship between total flash counts and the size of Larsen areas for flashes in general, it is rather weak. This is likely because all flashes associated with each Larsen area are considered in the flash count rather than just flashes inside the Larsen area. Many lightning flashes can occur outside Larsen areas in a maturing system, for example, despite its weakening state. The correlations between Larsen area size and stratiform and anvil flash count are even weaker, particularly since both types are associated with relatively weak convection, and local charging mechanisms can be significant sources of charge. Similar trends are examined for a number of convective proxies such as Larsen area minimum 85 and 37 GHz PCTs, 20, 30, and 40 dbZ echo tops, and maximum storm height (figures not shown), however, the correlations between these proxies and flash count are also insignificant, and so a more refined approach is needed to examine these relationships in depth.

4. Conclusions and Closing Remarks

[33] A global set of TRMM-based lightning statistics is presented that provides new insight into the occurrence of lightning in the stratiform and anvil regions of storms. Both types are shown to account for roughly 5% of all lightning, but 15–17% of areas where charge separation is likely, identified using contiguous area of echoes exceeding 30 dbZ at 6 km, are associated with at least one flash of either type. While more lightning occurs over land than over the ocean, stratiform flashes are shown to account for a larger fraction of lightning over the ocean than over land, including regions off the leeward coast of major continents. Anvil flashes account for a relatively high fraction of lightning flashes over high-terrain regions and arid regions. There are also substantial diurnal and seasonal variations in the frequency of stratiform and anvil flashes. The stratiform lightning fraction is higher during the winter in the subtropics, while the anvil flash fraction peaks during the summer. This trend is not as pronounced in the Southern Hemisphere where the anvil flashes over Argentina and the southern Atlantic are not included owing to interference from the South Atlantic Anomaly. Stratiform flashes also tend to be more common in the late afternoon and early morning over land while there is not much difference between the diurnal cycles of each type of lightning over the ocean, which is consistent with past studies of the diurnal cycles of the large MCSs.

[34] Anvil flashes often occur in regions near the edge of storm systems, and 65% are centered in regions with no detectible PR echo. Both stratiform and anvil flashes tend to occur near a relatively weak Larsen area. Larsen areas with stratiform flashes tend to be weaker than those with anvil flashes based on PR-based convective proxies, yet slightly based on TMI and VIRS proxies. We speculate that Larsen areas associated with anvil lightning are often in the early stage of convection with relatively small convective cores containing smaller amounts of ice particles, but sizable amounts of liquid and mixed-phase precipitation leading to relatively strong PR echoes. At the same time, Larsen areas associated with stratiform lightning may be in the mature stage of the convection, and occur in systems composed of multiple small Larsen areas.

[35] The strength of nearby Larsen areas as a function of flash count is also examined for each type of lightning. There is a weak relationship between Larsen area size and flash count for lightning in general, and the relationships are significantly weaker for stratiform and anvil flash count. This lack of a clear trend is likely due to the snapshot nature of TRMM data, deficiencies in our flash-to-Larsen area associations, and charge generation from in situ processes. Because of this, a more in-depth methodology is needed to relate lightning flashes to nearby charging regions and to examine stratiform and anvil flash initiation throughout the life of convective storms. Moreover, these results may not apply to winter storms in the subtropics since they are not considered in this study. Future work will combine TRMM data with observations from ground-based radars and lightning detection networks to further examine these statistical tendencies.

[36] **Acknowledgments.** Thanks are due to the three anonymous reviewers, as well as to Edward Zipser, who provided valuable comments and suggestions that greatly improved the quality of this paper. This research was supported by NASA grant NNX11AG31G under the direction of Erich Stocker. Thanks also go to John Kwiatkowski and the rest of the TRMM Science Data and Information System at NASA Goddard Space Flight Center, Greenbelt, Maryland, for data processing assistance.

References

Awaka, J., T. Iguchi, and K. Okamoto (1998), Rain type classification algorithm, *Meas. Precip. Space*, *3*, 213–224.

Battan, L. J. (1964), Some observations of vertical velocities and precipitation sizes in a thunderstorm, *J. Appl. Meteorol.*, *3*, 415–420, doi:10.1175/1520-0450(1964)003<0415:SOOVVA>2.0.CO;2.

Bluestein, H. B., and D. R. MacGorman (1998), Evolution of cloud-to-ground lightning characteristics and storm structure in the Spearman, Texas, tornadic supercells of 31 May 1990, *Mon. Weather Rev.*, *126*, 1451–1467, doi:10.1175/1520-0493(1998)126<1451:EOCTGL>2.0.CO;2.

Boccippio, D. J. W., J. Koshak, and R. J. Blakeslee (2002), Performance assessment of the Optical Transient Detector and Lightning Imaging Sensor. Part I: Predicted diurnal variability, *J. Atmos. Oceanic Technol.*, *19*, 1318–1332.

Bruning, E., W. D. Rust, T. J. Schuur, D. R. MacGorman, P. R. Krehbiel, and W. Rison (2007), Electrical and polarimetric radar observations of a multicell storm in TELEX, *Mon. Weather Rev.*, *135*, 2525–2544, doi:10.1175/MWR3421.1.

Carey, L. D., and S. A. Rutledge (2000), The relationship between precipitation and lightning in tropical island convection: A C-band polarimetric study, *Mon. Weather Rev.*, *128*, 2687–2710, doi:10.1175/1520-0493(2000)128<2687:TRBPAL>2.0.CO;2.

Carey, L. D., M. J. Murphy, T. L. McCormick, and N. W. S. Demetriades (2005), Lightning location relative to storm structure in a leading-line,

trailing-stratiform mesoscale convective system, *J. Geophys. Res.*, *110*, D03105, doi:10.1029/2003JD004371.
Cecil, D. J., S. J. Goodman, D. J. Boccippio, E. J. Zipser, and S. W. Nesbitt (2005), Three years of TRMM precipitation features. Part I: Radar, radiometric, and lightning characteristics, *Mon. Weather Rev.*, *133*, 543–566, doi:10.1175/MWR-2876.1.
Christian, H. J., et al. (2000), Algorithm theoretical basis document (ATBD) for the lightning imaging sensor (LIS), report, 53 pp., NASA, Greenbelt, Md.
Christian, H. J., et al. (2003), Global frequency and distribution of lightning as observed from space by the Optical Transient Detector, *J. Geophys. Res.*, *108*(D1), 4005, doi:10.1029/2002JD002347.
Dotzek, N., R. M. Rabin, L. D. Carey, D. R. MacGorman, T. L. McCormick, N. W. Demetriades, M. J. Murphy, and R. L. Holle (2005), Lightning activity related to satellite and radar observations of a mesoscale convective system over Texas on 7–8 April 2002, *Atmos. Res.*, *76*, 127–166, doi:10.1016/j.atmosres.2004.11.020.
Dye, J. E., et al. (2007), Electric fields, cloud microphysics, and reflectivity in anvils of Florida thunderstorms, *J. Geophys. Res.*, *112*, D11215, doi:10.1029/2006JD007550.
Ely, B. L., R. E. Orville, L. D. Carey, and C. L. Hodapp (2008), Evolution of the total lightning structure in a leading-line, trailing-stratiform mesoscale convective system over Houston, Texas, *J. Geophys. Res.*, *113*, D08114, doi:10.1029/2007JD008445.
Fu, Y., and G. Liu (2007), Possible misidentification of rain type by TRMM PR over Tibetan plateau, *J. Appl. Meteorol. Climatol.*, *46*, 667–672, doi:10.1175/JAM2484.1.
Hendon, H., and K. Woodberry (1993), The diurnal cycle of tropical convection, *J. Geophys. Res.*, *98*, 16,623–16,637, doi:10.1029/93JD00525.
Iguchi, T., T. Kozu, R. Meneghini, J. Awaka, and K. Okamoto (2000), Rain-profiling algorithm for the TRMM precipitation radar, *J. Appl. Meteorol.*, *39*, 2038–2052, doi:10.1175/1520-0450(2001)040<2038:RPAFTT>2.0.CO;2.
Jayaratne, E. R., C. P. R. Saunders, and J. Hallet (1983), Laboratory studies of the charging of soft hail during ice crystal interactions, *Q. J. R. Meteorol. Soc.*, *109*, 609–630, doi:10.1002/qj.49710946111.
Keighton, S. J., H. B. Bluestein, and D. R. MacGorman (1991), The evolution of a severe mesoscale convective system: Cloud-to-ground lightning location and storm structure, *Mon. Weather Rev.*, *119*, 1533–1556, doi:10.1175/1520-0493(1991)119<1533:TEOASM>2.0.CO;2.
Kuhlman, K. M., D. R. MacGorman, M. I. Biggerstaff, and P. R. Kreibiel (2009), Lightning initiation in the anvils of two supercell storms, *Geophys. Res. Lett.*, *36*, L07802, doi:10.1029/2008GL036650.
Kummerow, C., W. Barnes, T. Kozu, J. Shiue, and J. Simpson (1998), The Tropical Rainfall Measuring Mission (TRMM) sensor package, *J. Atmos. Oceanic Technol.*, *15*, 809–817, doi:10.1175/1520-0426(1998)015<0809:TTRMMT>2.0.CO;2.
Lang, T. J., and S. A. Rutledge (2008), Kinematic, microphysical, and electrical aspects of an asymmetric bow-echo mesoscale convective system observed during STEPS 2000, *J. Geophys. Res.*, *113*, D08213, doi:10.1029/2006JD007709.
Lang, T. J., S. A. Rutledge, and K. C. Wiens (2004), Origins of positive cloud-to-ground lightning flashes in the stratiform region of a mesoscale convective system, *Geophys. Res. Lett.*, *31*, L10105, doi:10.1029/2004GL019823.
Lang, T. J., W. A. Lyons, S. A. Rutledge, J. D. Meyer, D. R. MacGorman, and S. A. Cummer (2010), Transient luminous events above two mesoscale convective systems: Storm structure and evolution, *J. Geophys. Res.*, *115*, A00E22, doi:10.1029/2009JA014500.
Larsen, H. R., and E. J. Stansbury (1974), Association of lightning flashes with precipitation cores extending to height 7 km, *J. Atmos. Terr. Phys.*, *36*, 1547–1553, doi:10.1016/0021-9169(74)90232-3.
Liu, C., and E. J. Zipser (2008), Diurnal cycles of precipitation, clouds, and lightning in the tropics from 9 years of TRMM observations, *Geophys. Res. Lett.*, *35*, L04819, doi:10.1029/2007GL032437.
Lund, N. R., D. R. MacGorman, T. J. Schuur, M. I. Biggerstaff, and W. D. Rust (2009), Relationships between lightning location and polarimetric radar signatures in a small mesoscale convective system, *Mon. Weather Rev.*, *137*, 4151–4170, doi:10.1175/2009MWR2860.1.
MacGorman, D. R., W. D. Rust, P. Krehbiel, W. Rison, E. Bruning, and K. Weins (2005), The electrical structure of two supercell storms during STEPS, *Mon. Weather Rev.*, *133*, 2583–2607, doi:10.1175/MWR2994.1.
Marshall, J. S., and S. Radhakant (1978), Radar precipitation maps as lightning indicators, *J. Appl. Meteorol.*, *17*, 206–212, doi:10.1175/1520-0450(1978)017<0206:RPMALI>2.0.CO;2.
Marshall, T. C., and W. D. Rust (1993), Two types of vertical electrical structures in stratiform precipitation regions of mesoscale convective systems, *Bull. Am. Meteorol. Soc.*, *74*, 2159–2170, doi:10.1175/1520-0477(1993)074<2159:TTOVES>2.0.CO;2.
Marshall, T. C., W. D. Rust, W. P. Winn, and K. E. Gilbert (1989), Electrical structure in two thunderstorm anvil clouds, *J. Geophys. Res.*, *94*, 2171–2181, doi:10.1029/JD094iD02p02171.
Marshall, T. C., M. Stolzenburg, P. R. Krehbiel, N. R. Lund, and C. R. Maggio (2009), Electrical evolution during the decay stage of New Mexico thunderstorms, *J. Geophys. Res.*, *114*, D02209, doi:10.1029/2008JD010637.
Nesbitt, S. W., and E. J. Zipser (2003), The diurnal cycle of rainfall and convective intensity according to three years of TRMM measurements, *J. Clim.*, *16*, 1456–1475, doi:10.1175/1520-0442-16.10.1456.
Petersen, W. A., H. J. Christian, and S. A. Rutledge (2005), TRMM observations of the global relationship between ice water content and lightning, *Geophys. Res. Lett.*, *32*, L14819, doi:10.1029/2005GL023236.
Rutledge, S. A., and D. R. MacGorman (1988), Cloud-to-ground lightning activity in the 10–11 June 1985 mesoscale convective system observed during the Oklahoma-Kansas PRESTORM project, *Mon. Weather Rev.*, *116*, 1393–1408, doi:10.1175/1520-0493(1988)116<1393:CTGLAI>2.0.CO;2.
Saunders, C. P. R., W. D. Keith, and R. P. Mitzeva (1991), The effect of liquid water content on thunderstorm charging, *J. Geophys. Res.*, *96*, 11,007–11,017, doi:10.1029/91JD00970.
Schultz, D. M. (1999), Lake-effect snowstorms in northern Utah and western New York with and without Lightning, *Weather Forecasting*, *14*, 1023–1031, doi:10.1175/1520-0434(1999)014<1023:LESINU>2.0.CO;2.
Schuur, T. J., and S. A. Rutledge (2000), Electrification of stratiform regions in mesoscale convective systems. Part II: Two-dimensional numerical model simulations of a symmetric MCS, *J. Atmos. Sci.*, *57*, 1983–2006, doi:10.1175/1520-0469(2000)057<1983:EOSRIM>2.0.CO;2.
Spencer, R. W., H. G. Goodman, and R. E. Hood (1989), Precipitation retrieval over land and ocean with the SSM/I: Identification and characteristics of the scattering signal, *J. Atmos. Oceanic Technol.*, *6*, 254–273, doi:10.1175/1520-0426(1989)006<0254:PROLAO>2.0.CO;2.
Stolzenburg, M., T. C. Marshall, W. D. Rust, and B. F. Smull (1994), Horizontal distribution of electrical and meteorological conditions across the stratiform region of a mesoscale convective system, *Mon. Weather Rev.*, *122*, 1777–1797, doi:10.1175/1520-0493(1994)122<1777:HDOEAM>2.0.CO;2.
Stolzenburg, M., T. C. Marshall, and P. R. Krehbiel (2010), Duration and extent of large electric fields in a thunderstorm anvil cloud after the last lightning, *J. Geophys. Res.*, *115*, D19202, doi:10.1029/2010JD014057.
Takahashi, T. (1978), Riming electrification as a charge generation mechanism in thunderstorms, *J. Atmos. Sci.*, *35*, 1536–1548, doi:10.1175/1520-0469(1978)035<1536:REAACG>2.0.CO;2.
Takayabu, Y. N. (2006), Rain yield per flash calculated from TRMM PR and LIS data and its relationship to the contribution of tall convective rain, *Geophys. Res. Lett.*, *33*, L18705, doi:10.1029/2006GL027531.
Xu, W., E. J. Zipser, C. Liu, and H. Jiang (2010), On the relationships between lightning frequency and thundercloud parameters of regional precipitation systems, *J. Geophys. Res.*, *115*, D12203, doi:10.1029/2009JD013385.
Yamamoto, M. K., A. Higuchi, and K. Nakamura (2006), Vertical and horizontal structure of winter precipitation systems over the western Pacific around Japan using TRMM data, *J. Geophys. Res.*, *111*, D13108, doi:10.1029/2005JD006412.

C. Liu and M. Peterson, Department of Atmospheric Sciences, University of Utah, 135 S 1460 E, Room 819, Salt Lake City, UT 84112-0110, USA. (michael.j.peterson@utah.edu)